Available online at www.sciencedirect.com
SCIENCE DIRECT®
Journal of the European Ceramic Society 25 (2005) 793–799
www.elsevier.com/locate/jeurceramsoc

Crystal structure of rare-earth silicon-oxynitride J-phases, $Ln_4Si_2O_7N_2$

Junichi Takahashi [a,*], Hisanori Yamane [b], Naoto Hirosaki [c], Yoshinobu Yamamoto [c], Mamoru Mitomo [c], Masahiko Shimada [a]

[a] *Institute of Multidisciplinary Research for Advanced Materials, Tohoku University, Sendai 980-8577, Japan*
[b] *Center for Interdisciplinary Research, Tohoku University, Sendai 980-8578, Japan*
[c] *National Institute for Materials Science, Tsukuba 305-0044, Japan*

Received 5 September 2003; received in revised form 5 February 2004; accepted 13 February 2004
Available online 20 June 2004

Abstract

Rare-earth silicon-oxynitride J-phases, $Ln_4Si_2O_7N_2$ (Ln = Y, La, Pr, Nd, Sm, Gd, Tb, Dy, Ho, Er, Tm, Yb, and Lu), were prepared by the N_2 gas-pressured sintering method at 1 MPa of N_2 and 1500–1700 °C. The Rietveld analysis was carried out for X-ray powder diffraction data measured at room temperature. The crystal structures of $Ln_4Si_2O_7N_2$ were refined with the structure model of $La_4Si_2O_7N_2$ for Ln = La, Pr, Nd, and Sm, and with that of $Lu_4Si_2O_7N_2$ for Ln = Y, Gd, Tb, Dy, Ho, Er, Tm, Yb, and Lu. The refined monoclinic unit-cell parameters (lengths *a*, *b*, *c*, angles β, and volume *V*) increased linearly in their two series of Ln with increasing ionic radii of rare-earth atoms. Discontinuities of the unit-cell parameters were found between the two Ln series.

Keywords: Powders-solid-state reaction; X-ray methods; Rare-earth silicon-oxynitrides; $Ln_4Si_2O_7N_2$

1. Introduction

Rare-earth oxide additives have been used for sintering of non-oxide structural materials, such as Si_3N_4, AlN, and SiC. Recently, some of the authors reported that the flexural strengths of the hot-pressed sintered Si_3N_4 ceramics containing the additive of Yb_2O_3[1–3] or Lu_2O_3[4,5] were higher than those of the ceramics containing other rare-earth oxide additives. The rare-earth silicon-oxynitrides of $Yb_4Si_2O_7N_2$ and $Lu_4Si_2O_7N_2$ were found at the grain boundaries in the high-flexural strength ceramics. These oxynitrides are so-called J-phases.

From the later half of 1970s to the end of 1990s, single phases of $Ln_4Si_2O_7N_2$ (Ln = Y and rare-earth elements, except Pm and Eu) were prepared and the monoclinic unit-cell parameters were reported.[6–20] In these studies using X-ray diffraction method, the crystal structures of the $Ln_4Si_2O_7N_2$ series were considered to have a cuspidine ($Ca_4Si_2O_7F_2$) type. Recently, we measured the time-of-flight (TOF) neutron powder diffraction data of $La_4Si_2O_7N_2$[21] and $Lu_4Si_2O_7N_2$[22,23] synthesized, and refined their structural parameters (unit-cell parameters, atomic coordinates, and occupancies of oxygen and nitrogen atoms in the nonmetal sites) by the Rietveld analysis. The results indicated that $Lu_4Si_2O_7N_2$ has the cuspidine-type structure, but $La_4Si_2O_7N_2$ has a cuspidine-related structure. The difference of the two structures is the stacking of atomic packages (volume of $a \times b/2 \times c$) along the unique *b*-axis, as shown in Fig. 1. The typical difference is an arrangement of $Si_2(O,N)_7$ ditetrahedra drawn with hatched line in Fig. 1 that the ditetrahedra form a zigzag line in $La_4Si_2O_7N_2$ and a parallel one in $Lu_4Si_2O_7N_2$, although both $La_4Si_2O_7N_2$ and $Lu_4Si_2O_7N_2$ have the same space group (monoclinic, $P2_1/c$), and all atoms are situated at the general positions (4e) in the structures. In addition, our refined unit-cell parameters of $La_4Si_2O_7N_2$ and $Lu_4Si_2O_7N_2$ were significantly different from those reported previously.[6–9,12,13]

These situations motivated us to reevaluate the crystal structure of the series of J-phases, $Ln_4Si_2O_7N_2$, with various rare-earth elements. In the present study, we prepared $Ln_4Si_2O_7N_2$ with Ln = Y, La, Pr, Nd, Sm, Gd, Tb, Dy, Ho, Er, Tm, Yb, and Lu, and investigated the crystal structures of the J-phases by the Rietveld method using the X-ray powder diffraction (XRPD) data.

* Corresponding author. Tel.: +81-22-217-5161; fax: +81-22-217-5160.
E-mail address: junichi@tagen.tohoku.ac.jp (J. Takahashi).

0955-2219/$ – see front matter © 2004 Elsevier Ltd. All rights reserved.
doi:10.1016/j.jeurceramsoc.2004.02.008

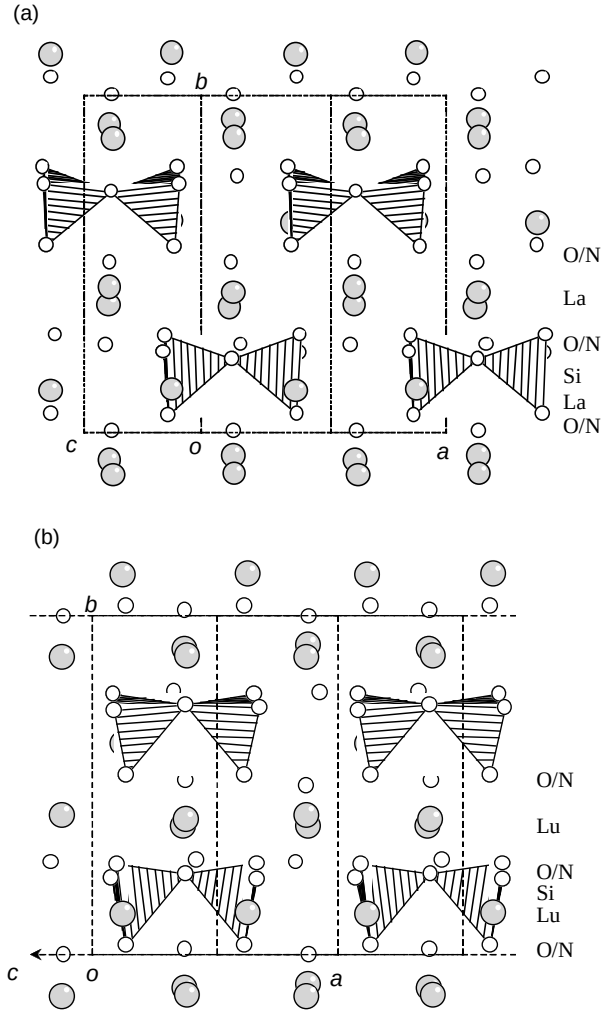

Fig. 1. Projection views of the crystal structure of (a) $La_4Si_2O_7N_2$, and (b) $Lu_4Si_2O_7N_2$ on the *a*–*b* plane ($z = -0.1$ to 0.6). Two hatched $Si(O,N)_4$ tetrahedra form $Si_2(O,N)_7$ ditetrahedra.

2. Experimental

2.1. Sample preparation

The powders of α-Si_3N_4 (SN-E10, UBE Industries, Tokyo, Japan), SiO_2 (99.9%, Kojundo Chemical Lab. Co. Ltd., Sakado, Japan), and rare-earth oxides, Ln_2O_3 (Ln = Y, La, Nd, Sm, Gd, Dy, Ho, Er, Tm, Yb, Lu; 99.9%, Shin-Etsu Chemical Co. Ltd., Tokyo, Japan), Pr_6O_{11} (99.9%, Shin-Etsu Chemical Co. Ltd.), and Tb_4O_7 (99.9%, Shin-Etsu Chemical Co. Ltd.) were used for sample preparation. Before weighing, the rare-earth oxides were heated at 1000 °C for 4 h in air. The powders weighed in stoichiometry (total ca. 10 g) were mixed in a silicon nitride ball-mill for 2 h with 100 ml of ethanol as a dispersant. The slurry mixture was dried in a rotary evaporator and 2 g of the powder was pressed into a 12 mm ϕ pellet. The pellet was then put into a high-purity boron nitride crucible, and heated in a gas-pressured sintering furnace (FVPHR-R-10, FRET-40, Fujidempa Kogyo Co. Ltd., Osaka, Japan) with a graphite heater. The sample was heated at a constant heating rate of 600 °C h^{-1} under 10^{-2} Pa in vacuum from room temperature to 800 °C. At this temperature, a nitrogen gas (99.999% purity) was introduced in the furnace. Then, the sample was reheated at the same heating rate and maintained at 1500 °C for 8 h, 1600 °C for 8 h, or 1700 °C for 4 h under a nitrogen gas pressure of 1 MPa. After heating, the sample was cooled at a constant rate of −600 °C h^{-1} to 1200 °C, and then cooled slowly without temperature control in the furnace.

2.2. Diffraction measurements and structure analysis

A reaction-sintered sample was crushed in an agate mortar, and was offered to the XRPD experiment which was performed at room temperature on a diffractometer system equipped with a pyrolytic graphite monochromator (Rigaku RINT 2500V) using Cu Kα radiation. The XRPD pattern was measured over a 2θ range from 10 to 130° with a step width of 0.03° and a counting time of 1 s per step.

The Rietveld analysis was carried out using a program RIETAN-2000.[24] The structural parameters of $La_4Si_2O_7N_2$[21] and $Lu_4Si_2O_7N_2$[22] refined by the neutron powder diffraction data were used as structure models in

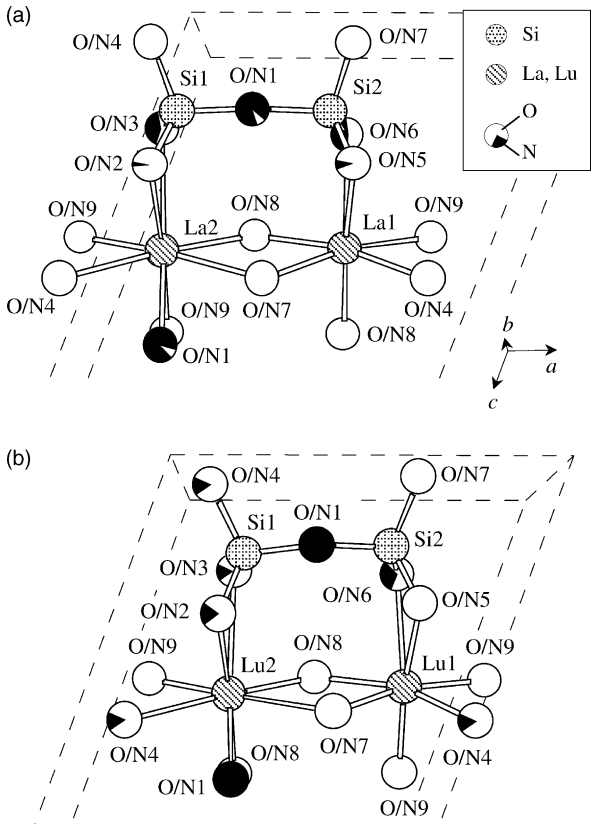

Fig. 2. A part of crystal structure of (a) $La_4Si_2O_7N_2$ ($y = -0.06$ to 0.35)[21] and (b) $Lu_4Si_2O_7N_2$ ($y = -0.03$ to 0.27)[22] projected on the *a*–*c* plane. Areas drawn with white and black colors in the non-metal sites refer to the occupancies of oxygen and nitrogen atoms, respectively.

Table 1
Unit-cell parameters and volumes of $Ln_4Si_2O_7N_2$ ($P2_1/c$) refined by the Rietveld analysis of X-ray diffraction data, and *R*-factors

Ln	Unit-cell parameters ($P2_1/c$)					*R*-factors							Preparation temperature/°C	Second phase[a]
	a/Å	*b*/Å	*c*/Å	*β*/°	Unit-cell volume/Å^3	R_{wp}	R_p	R_R	R_e	S	R_I	R_F		
Y	7.5620(5)	10.4639(5)	10.7361(7)	110.078(3)	797.90(8)	7.71	5.78	9.87	5.98	1.2894	2.01	1.15	1700	
La	8.0398(4)	10.9951(4)	11.1096(5)	110.929(3)	917.28(7)	8.90	6.37	8.08	7.05	1.2622	2.07	0.99	1500	
Pr	7.8964(5)	10.8159(6)	11.0210(7)	110.664(3)	880.71(9)	11.49	8.83	11.19	7.54	1.5239	4.32	2.61	1700	O
Nd	7.8488(4)	10.7386(5)	10.9982(6)	110.553(3)	867.98(8)	9.26	6.68	9.04	6.91	1.3400	2.01	1.03	1500	A
Sm	7.7514(4)	10.6293(4)	10.9347(5)	110.416(2)	844.34(7)	9.64	7.11	9.85	7.22	1.3350	3.21	1.50	1700	
Gd	7.6902(5)	10.6425(6)	10.8228(7)	110.358(3)	830.44(9)	8.35	6.34	9.84	6.08	1.3730	2.93	1.42	1700	A
Tb	7.6419(3)	10.5411(4)	10.8098(4)	110.207(2)	817.17(5)	9.62	7.44	12.05	6.95	1.3846	2.90	1.66	1700	O
Dy	7.6006(3)	10.5156(4)	10.7541(5)	110.195(2)	806.68(5)	10.32	7.68	10.23	7.59	1.3595	3.32	1.61	1700	
Ho	7.5637(4)	10.4481(5)	10.7577(6)	110.059(3)	798.58(7)	9.87	6.85	8.99	7.55	1.3077	1.92	1.21	1600	A
Er	7.5212(3)	10.4109(4)	10.7136(5)	109.999(2)	788.32(6)	8.73	6.49	8.65	7.26	1.2030	1.84	1.14	1700	
Tm	7.4892(3)	10.3547(4)	10.6892(5)	109.924(2)	779.32(6)	6.34	4.90	8.53	4.63	1.3689	2.02	1.19	1700	
Yb	7.4611(3)	10.3140(3)	10.6649(4)	109.892(2)	771.73(5)	9.76	7.07	8.54	7.58	1.2875	1.60	1.04	1700	
Lu	7.4201(3)	10.2743(3)	10.6548(4)	109.793(2)	764.29(5)	9.44	6.66	8.21	7.43	1.2710	2.14	1.48	1700	

[a] O: rare-earth oxides, A: apatite ($Ln_{10}(SiO_4)_6N_2$).

the Rietveld analysis. A part of the crystal structures of $La_4Si_2O_7N_2$ and $Lu_4Si_2O_7N_2$ projected on the *a*–*c* plane is shown in Fig. 2 in which the proportion of white and black area in the nonmetal sites represents the occupancies of oxygen and nitrogen (O/N) atoms, respectively. Because the O/N ratio scarcely affected on the refinement results using the XRPD data, the O/N occupancies were fixed to those reported for $La_4Si_2O_7N_2$ or $Lu_4Si_2O_7N_2$.

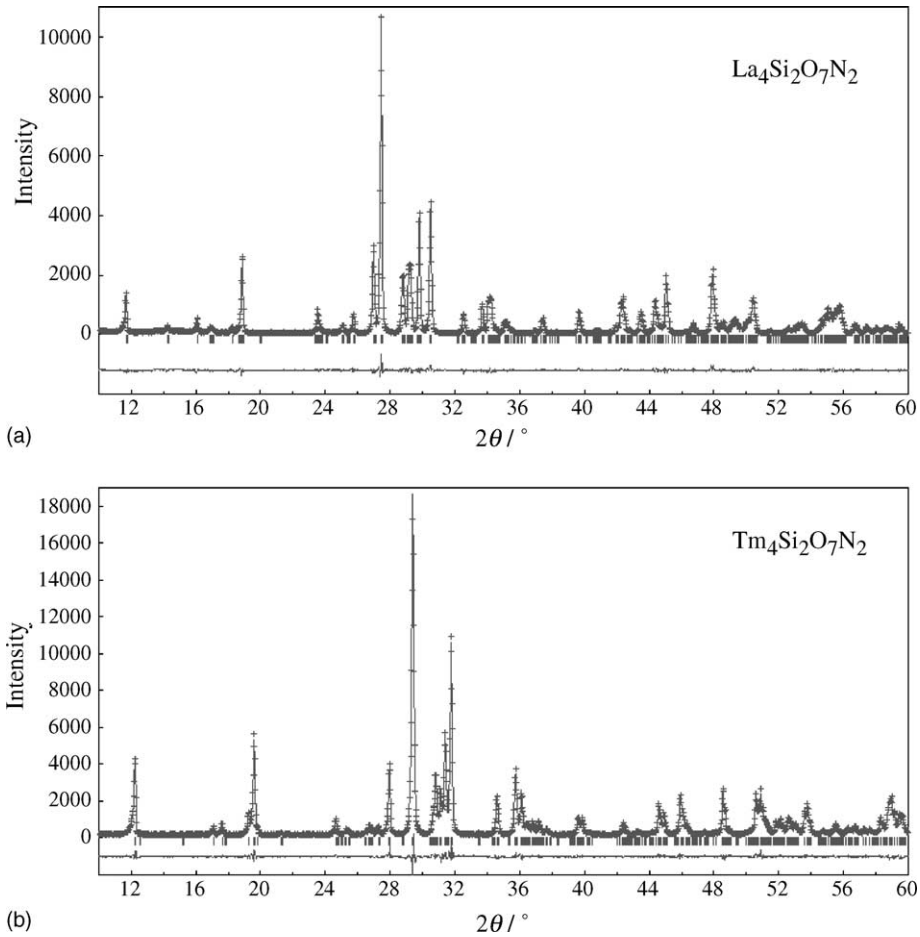

Fig. 3. X-ray powder diffraction patterns (Cu Kα) and Rietveld refinement profiles for (a) $La_4Si_2O_7N_2$ and (b) $Tm_4Si_2O_7N_2$. Observed (+), calculated (solid line), peak position (|), and differences.

3. Results and discussion

Single phases of $Ln_4Si_2O_7N_2$ were obtained for Ln = Y, La, Sm, Dy, Er, Tm, Yb, and Lu. Small amounts (<4 mass%) of apatite-type $Ln_{10}(SiO_4)_6N_2$ were included in the samples prepared with Ln = Nd, Gd, and Ho. When Pr_6O_{11} and Tb_4O_7 were used as starting materials, the J-phase yields about 90 mass%. In the case of Eu, no J-phase, but a mixture of oxides and/or oxynitrides was synthesized, as Montorsi and Appendino reported.[9] These facts suggest that formation of $Ln_4Si_2O_7N_2$ is related to the stability of trivalent Ln cations. Pr and Tb atoms can easily take various valence states other than 3+, and Eu^{2+} is stable in a reduced atmosphere.

The final results of the refined unit-cell parameters (lengths *a*, *b*, *c*, angle *β*, and volume *V*) of $Ln_4Si_2O_7N_2$ (monoclinic space group $P2_1/c$) are given in Table 1 together with the final *R*-values. The multi-phase Rietveld analysis was performed for the sample with Ln = Pr, Nd, Gd, Tb, and Ho. The structural parameters except for the scale factor and unit-cell parameters were fixed to the reported values for $Ln_{10}(SiO_4)_6N_2$,[25] Pr_2O_3,[26] and Tb_2O_3.[27] Fig. 3 shows examples of the observed and calculated XRPD patterns and their differences resulted from the Rietveld analysis. By adopting the $La_4Si_2O_7N_2$ structure model to $Ln_4Si_2O_7N_2$ with Ln = La, Pr, Nd, and Sm, and the $Lu_4Si_2O_7N_2$ model to those with Ln = Y, Gd, Tb, Dy, Ho, Er, Tm, Yb, and Lu, the structure of J-phases were refined well. When the

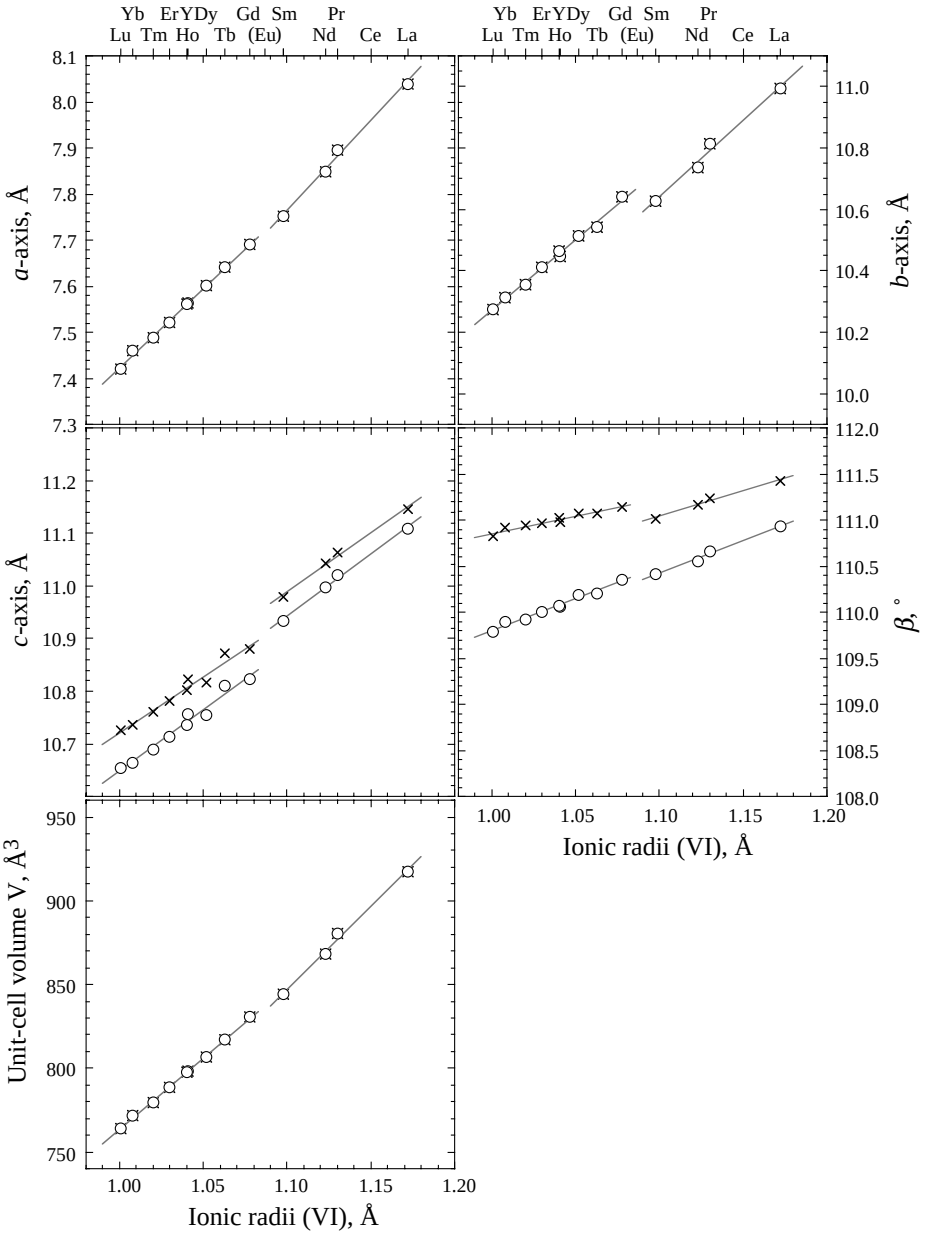

Fig. 4. Refined unit-cell parameters (lengths and angles) and volumes of $Ln_4Si_2O_7N_2$ as a function of the ionic radius of sixfold coordinated Ln^{3+}. The values with $P2_1/c$ cell and $P2_1/n$ cell are plotted with "○" and "×" marks, respectively.

other model was used in each group, *R*-values rose about 1% and interatomic distances between Si and O/N atoms remarkably scattered. For example, Si–O/N distances for $Er_4Si_2O_7N_2$ by using $Lu_4Si_2O_7N_2$ structure model ranged from 1.62 to 1.73 Å, but those by using $La_4Si_2O_7N_2$ model ranged from 1.33 to 2.02 Å. While *R*-factors and interatomic distances vary depending on the structure model, it is to be noted that the refined unit-cell parameters between two structure models are close each other. For $Er_4Si_2O_7N_2$, the parameters of $a = 7.5212(3)$ Å, $b = 10.4109(4)$ Å, $c = 10.7136(5)$ Å, and $\beta = 109.999(2)^\circ$ are obtained from $Lu_4Si_2O_7N_2$ model and those of $a = 7.5220(4)$ Å, $b = 10.4121(4)$ Å, $c = 10.7150(6)$ Å, and $\beta = 109.998(3)^\circ$ from $La_4Si_2O_7N_2$ model.

Fig. 4 plots the refined unit-cell parameters of $Ln_4Si_2O_7N_2$ listed in Table 1 against the ionic radii[28] of sixfold coordinated Ln^{3+}. When the twofold symmetric axis of the monoclinic cell is taken in the *b*-axis (unique axis), there are three possible cell choices of $P2_1/c$, $P2_1/n$, and $P2_1/a$.[19,23,29] In the structure refinement in this work, we chose the $P2_1/c$ cell in accordance with "cell choice 1" in the International Tables.[29]

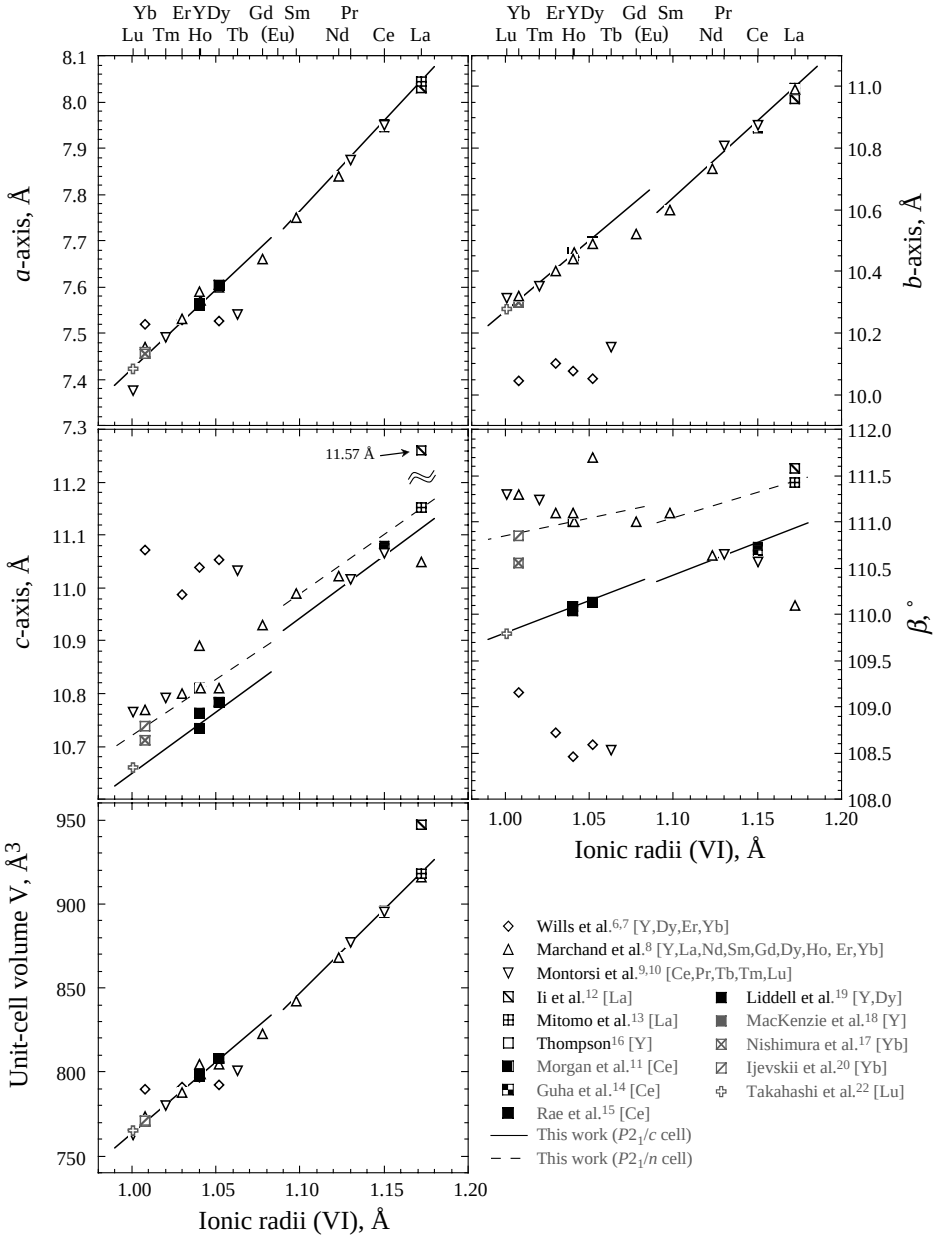

Fig. 5. Unit-cell parameters (lengths and angles) and volumes of $Ln_4Si_2O_7N_2$ reported in the literatures vs. the ionic radius of sixfold coordinated Ln^{3+}. The results of the present study are shown with solid lines ($P2_1/c$ cell) and broken lines ($P2_1/n$ cell). (◇) Wills et al.[6,7] [Y, Dy, Er, Yb]; (△) Marchand et al.[8] [Y, La, Nd, Sm, Gd, Dy, Ho, Er, Yb]; (▽) Montorsi and Appendino[9,10] [Ce, Pr, Tb, Tm, Lu]; (▧) Ii et al.[12] [La]; (□) Liddell et al.[19] [Y, Dy]; (⊞) Mitomo et al.[13] [La]; (◩) MacKenzie et al.[18] [Y]; (□) Thompson[16] [Y]; (⊠) Nishimura and Mitomo[17] [Yb]; (◧) Morgan[11] [Ce]; (▨) Ijevskii et al.[20] [Yb]; (◪) Guha[14] [Ce]; (✣) Takahashi et al.[22] [Lu]; (■) Rae et al.[15] [Ce]; (—) this work ($P2_1/c$ cell); (- - -) this work ($P2_1/n$ cell).

As pointed out in the previous studies,[19,23] the values of the *c*-axis length and β angles of the $P2_1/c$ cell are very close but different to those of $P2_1/n$ cell, whereas the *a*- and *b*-axes between the $P2_1/c$ and $P2_1/n$ cells are common. The relationships between the unit-cell parameters of $P2_1/c$ and $P2_1/n$ are expressed as follows:

$$a_n = a_c \quad (1)$$

$$b_n = b_c \quad (2)$$

$$c_n = (a_c^2 + c_c^2 + 2a_c c_c \cos\beta_c)^{1/2} \quad (3)$$

$$\beta_n = \cos^{-1}\left\{\frac{(c_c^2 - a_c^2 - c_n^2)}{(2a_c c_n)}\right\} \quad (4)$$

where subscripts *c* and *n* refer to the $P2_1/c$ and $P2_1/n$ cells, respectively. The *c*-axis lengths and β angles of the $P2_1/n$ cell converted from those of the $P2_1/c$ cell are plotted in Fig. 4 with the "×" marks. It can be seen from this figure that the differences of the *c*-axis lengths as well as the β angles between the $P2_1/c$ and $P2_1/n$ cells are small; for example, 0.037 Å and 0.494° for Ln = La and 0.071 Å and 0.950° for Ln = Lu.

The unit-cell lengths *a*, *b*, *c*, and angles β, and the unit-cell volumes *V* increased linearly with increasing ionic radii of rear-earth elements from 1.001 Å (Lu) to 1.078 Å (Gd) and from 1.098 Å (Sm) to 1.172 Å (La). Slopes of the straight lines fitted by the least-squares method from the corresponding data are different between the two groups of Ln = La to Sm and Ln = Y and Gd to Lu. The remarkable discontinuities or gaps of lines between Gd and Sm were seen for the *b*- and *c*-axis lengths. The *b*-axis length dropped and the *c*-axis length jumped up by a replacement of Gd with Sm.

It is interested that such Ln size dependence of the unit-cell parameters in the series of $Ln_4Si_2O_7N_2$ corresponds to the temperature dependence of the unit-cell parameters in $Y_4Al_2O_9$ with a high-temperature phase transition in which the low-temperature $Y_4Al_2O_9$ phase (space group $P2_1/c$) transforms to the high-temperature $Y_4Al_2O_9$ phase (space group $P2_1/c$) at around 1370 °C.[30,31] The unit-cell parameters of $Y_4Al_2O_9$ increase gradually with an increase of temperature, and, at the transition temperature, the unit-cell parameters change discontinuously with the decrease of the *a*- and *b*-axis lengths and the increase of the *c*-axis. The similarity of the unit-cell parameter changes observed in the series of $Ln_4Si_2O_7N_2$ and the phase transition of $Y_4Al_2O_9$ can be understood as a volume change of atomic sites by ionic radii or by thermal vibration. Although the critical cell volume for the structure change in the $Ln_4Si_2O_7N_2$ series has not been clarified in this work, a solid solution system, such as $(Gd,Sm)_4Si_2O_7N_2$, in which Ln atoms with ionic radii larger and smaller than Eu^{3+} ionic radius are combined may give the explanation.

Fig. 5 compiles the unit-cell parameters of $Ln_4Si_2O_7N_2$ reported in the previous studies. The results of the present study are represented with solid lines ($P2_1/c$ cell) and broken lines ($P2_1/n$ cell) in this figure. The unit-cell lengths of *a* and *b*, and volumes *V* are comparably plotted on the same lines except for the data for Ln = Y, Dy, Er, and Yb by Wills et al.[6,7] and for Ln = La by Ii et al.[12] Complemental and systematical investigation was performed by Marchand et al.[8] and Montorsi and Appendino[9,10] for the unit-cell parameters of $Ln_4Si_2O_7N_2$ with various rare-earth atoms. The values of the *c*-axis lengths and β angles reported by them seem to be closed to our results of the $P2_1/n$ cells at smaller Ln^{3+} ionic radii and to those of the $P2_1/c$ cells at larger ionic radii. These facts show an evidence of the errant indexing on the XRPD data in the previous studies where the crystal structures of $Ln_4Si_2O_7N_2$ were uncertain. Liddell et al. considered the choice of the unit cell ($P2_1/a$ or $P2_1/n$) for the J-phase with Ln = Y and Dy.[19] The $P2_1/a$ cells they reported were close to the $P2_1/c$ cells of ours by replacement of the *a*- and *c*-axes. The unit-cell parameters of $Y_4Si_2O_7N_2$[18] refined by the Rietveld method using the $P2_1/c$ cell agreed with our results within the standard deviation. From these comparisons, it was concluded that the unit-cell parameters of $Ln_4Si_2O_7N_2$ were obtained systematically with good precision in the present study.

4. Conclusions

The crystal structures of the rare-earth silicon-oxynitrides $Ln_4Si_2O_7N_2$ at room temperature were classified into two groups with Ln = La to Sm and with Ln = Gd to Lu and Y. These results were demonstrated not only by judging for the *R*-factors and interatomic distances given from the Rietveld refinement using the structure models of $La_4Si_2O_7N_2$ and $Lu_4Si_2O_7N_2$ whose structures had been determined with the neutron powder diffraction data, but also by a continual change of the monoclinic unit-cell parameters (lengths *a*, *b*, *c*, angles β, and volume *V*) refined with the $P2_1/c$ cell, which were plotted on the linear lines in each Ln group against the radii of the trivalent Ln cation. The clear gaps were revealed between the lines of the two groups. The liner change and the gaps of the unit-cell parameters with increasing Ln^{3+} radii for $Ln_4Si_2O_7N_2$ were analogous with the change of unit-cell parameters observed for $Y_4Al_2O_9$ with increasing temperature and at the high-temperature phase transition. The scattered unit-cell parameters of $Ln_4Si_2O_7N_2$ reported in the previous studies were probably due to indexing of the diffraction peaks with the assumption of the same cuspidine-type structure for all $Ln_4Si_2O_7N_2$ compounds and without any attention to the choice of the $P2_1/c$ cell and the $P2_1/n$ cell.

References

1. Nishimura, T., Mitomo, M. and Suematsu, H., High temperature strength of silicon nitride ceramics with ytterbium silicon oxynitride. *J. Mater. Res.* 1997, **12**, 203–209.

2. Park, H., Kim, H. E. and Niihara, K., Microstructural evolution and mechanical properties of Si_3N_4 with Yb_2O_3 as a sintering additive. *J. Am. Ceram. Soc.* 1997, **80**, 750–756.
3. Yamamoto, Y., Hirosaki, N., Nishimura, T. and Mitomo, M., Gas-pressure sintering of silicon nitride with $Yb_4Si_2O_7N_2$ phase. *J. Ceram. Soc. Jpn.* 2001, **109**, 453–456.
4. Hirosaki, N., Yamamoto, Y., Nishimura, T. and Mitomo, M., Japanese Patent No. 324327 (2000).
5. Guo, S., Hirosaki, N., Yamamoto, Y., Nishimura, T. and Mitomo, M., Improvement of high-temperature strength of hot-pressed sintering silicon nitride with Lu_2O_3 addition. *Scripta Mater.* 2001, **45**, 867–874.
6. Wills, R. R., Stewart, R. W., Cunningham, J. A. and Wimmer, J. M., The silicon lanthanide oxynitrides. *J. Mater. Sci.* 1976, **11**, 749–759.
7. Wills, R. R., Holmquist, S., Wimmer, J. M. and Cunningham, J. A., Phase relationships in the system Si_3N_4-Y_2O_3-SiO_2. *J. Mater. Sci.* 1976, **11**, 1305–1309.
8. Marchand, M. M. R., Jayaweera, A., Verdier, P. and Lang, J., Préparation et caractérisation de nouveaux oxynitrures dans le système Ln-Si-O-N. Les mélilites $Ln_2Si_3O_3N_4$ et les cuspidines $Ln_4Si_2O_7N_2$. *Compt. Rend. Acad. Sci. Paris Ser. C* 1976, **283**, 675–677.
9. Montorsi, M. and Appendino, P., Silicon lanthanide oxynitrides of the $M_4Si_2O_7N_2$ type. *J. Less Common Met.* 1979, **68**, 193–197.
10. Montorsi, M. and Appendino, P., Silicon terbium oxynitride of composition $Tb_4Si_2O_7N_2$. *Am. Ceram. Soc. Bull.* 1979, **58**, 789.
11. Morgan, P. E. D., Comment on the structures of $Ce_4Si_2O_7N_2$, $La_4Si_2O_7N_2$, "$Ce_2O_3{\cdot}2Si_3N_4$," and "$La_2O_3{\cdot}2Si_3N_4$". *J. Am. Ceram. Soc.* 1979, **62**, 636.
12. Ii, N., Mitomo, M. and Inoue, Z., Single-crystal growth of $La_4Si_2O_7N_2$ by the floating zone method. *J. Mater. Sci.* 1980, **15**, 1691–1965.
13. Mitomo, M., Izumi, F., Horiuchi, S. and Matsui, Y., Phase relationships in the system Si_3N_4-SiO_2-La_2O_3. *J. Mater. Sci.* 1982, **17**, 2359–2364.
14. Guha, J. P., The crystal structure of the silicon cerium oxynitride, $Ce_4Si_2O_7N_2$. *J. Mater. Sci.* 1980, **15**, 262–263.
15. Rae, A. W. J. M., Buang, K. B. and Thompson, D. P., Comment on "The crystal structure of the silicon cerium oxynitride $Ce_4Si_2O_7N_2$". *J. Mater. Sci.* 1980, **15**, 264–265.
16. Thompson, D. P., Tailoring multiphase and composite ceramics. *Materials science research* (*Vol. 20*), Plenum, New York, 1986.
17. Nishimura, T. and Mitomo, M., Phase relationships between the system Si_3N_4-SiO_2-Yb_2O_3. *J. Mater. Res.* 1995, **10**, 240–242.
18. MacKenzie, K. J. D., Gaonsfold, G. J. and Tyan, M. J., Rietveld refinement of the crystal structure of the yttrium silicon oxynitrides $Y_2Si_3O_3N_4$ (N-melilite) and $Y_4Si_2O_7N_2$ (J-phase). *J. Eur. Ceram. Soc.* 1996, **16**, 553–560.
19. Liddell, K., Thompson, D. P., Wang, P. L., Sum, W. Y., Gao, L. and Yan, D. S., J-phase solid solution series in the Dy-Si-Al-O-N system. *J. Eur. Ceram. Soc.* 1998, **18**, 1479–1492.
20. Ijevskii, V. A., Kolitsch, U., Seifert, H. J., Wiedmann, I. and Aldinger, F., Aluminum-containing ytterbium nitrogen woehlerite solid solutions. Synthesis, structure, and some properties. *J. Eur. Ceram. Soc.* 1998, **18**, 543–552.
21. Takahashi, J., Yamane, H., Hirosaki, N., Yamamoto, Y., Suehiro, T., Kamiyama, T. *et al.*, Crystal structure of $La_4Si_2O_7N_2$ analyzed by the Rietveld method using the time-of-flight neutron powder diffraction data. *Chem. Mater.* 2003, **15**, 1099–1104.
22. Takahashi, J., Yamane, H., Shimada, M., Yamamoto, Y., Hirosaki, N., Mitomo, M. *et al.*, Crystal structure of $Lu_4Si_2O_7N_2$ analyzed by the Rietveld method of time-of-flight neutron powder diffraction pattern. *J. Am. Ceram. Soc.* 2002, **85**, 2072–2077.
23. Takahashi, J., Yamane, H., Yamamoto, Y., Hirosaki, N., Mitomo, M., Oikawa, K. *et al.*, Ordering of oxygen and nitrogen in J-phase $Lu_4Si_2O_7N_2$. *Key Eng. Mater.* 2003, **237-237**, 53–58.
24. Izumi, F., *The Rietveld method*. Oxford University Press, Oxford, 1995.
25. Titeux, S., Gervais, M., Verdier, P. and Laurent, Y., Synthesis and X-ray diffraction study of substituted $La_{10}(Si_6O_{22}N_2)O_2$ silicon apatites. *Mater. Sci. Forum* 2000, **325/326**, 17–20.
26. Wolf, R. and Hoppe, R., Eine notiz zum A-typ lanthanoidoxide: ueber Pr_2O_3. *Z. Anorg. Allgem. Chem.* 1985, **529**, 61–64.
27. Saiki, A., Ishizawa, N., Mizutani, N. and Kato, M., Structural change of C-type rare earth oxides, ytterbium oxide and erbium oxide at high temperatures. *J. Ceram. Soc. Jpn.* 1985, **93**, 649–654.
28. Shannon, R. D., Revised effective ionic radii and systematic studies of interatomic distances in halides and chalcogenides. *Acta Crystallogr.* 1976, **A32**, 751–767.
29. *International Tables for crystallography* (*Vol. A*), 4th revised ed. The Netherlands, 1996.
30. Yamane, H., Omori, M., Okubo, A. and Hirai, T., High-temperature phase transition of $Y_4Al_2O_9$. *J. Am. Ceram. Soc.* 1993, **76**, 2382–2384.
31. Yamane, H., Shimada, M. and Hunter, B. A., High-temperature neutron diffraction study of $Y_4Al_2O_9$. *J. Solid State Chem.* 1998, **141**, 466–474.